Exogenous Expression of the Amino-terminal Half of the Tight Junction Protein ZO-3 Perturbs Junctional Complex Assembly

Erika S. Wittchen, Julie Haskins, and Bruce R. Stevenson

Department of Cell Biology, University of Alberta, Edmonton, Alberta, Canada T6G 2H7

Abstract. The functional characteristics of the tight junction protein ZO-3 were explored through exogenous expression of mutant protein constructs in MDCK cells. Expression of the amino-terminal, PSD95/dlg/ZO-1 domain-containing half of the molecule (NZO-3) delayed the assembly of both tight and adherens junctions induced by calcium switch treatment or brief exposure to the actin-disrupting drug cytochalasin D. Junction formation was monitored by transepithelial resistance measurements and localization of junction-specific proteins by immunofluorescence. The tight junction components ZO-1, ZO-2, endogenous ZO-3, and occludin were mislocalized during the early stages of tight junction assembly. Similarly, the adherens junction proteins E-cadherin and β-catenin were also delayed in their recruitment to the cell membrane, and NZO-3 expression had striking effects on actin cytoskeleton dynamics. NZO-3 expression did not alter expression levels of ZO-1, ZO-2, endogenous ZO-3, occludin, or E-cadherin; however, the amount of Triton X-100–soluble, signaling-active β-catenin was increased in NZO-3–expressing cells during junction assembly. In vitro binding experiments showed that ZO-1 and actin preferentially bind to NZO-3, whereas both NZO-3 and the carboxy-terminal half of the molecule (CZO-3) contain binding sites for occludin and cingulin. We hypothesize that NZO-3 exerts its dominant-negative effects via a mechanism involving the actin cytoskeleton, ZO-1, and/or β-catenin.

Key words: zonula occludens-3 protein • tight junction • cadherins • actin cytoskeleton • β-catenin

Introduction

Regulated transport of substances across a polarized epithelial cell sheet occurs via two distinct routes: the transcellular pathway, where substances are vectorially transported through the cytoplasm (transcytosis); and the paracellular pathway, where molecules selectively pass through the spaces between adjoining cells. The tight junction (TJ)[1] is the structural element that forms a physical barrier to the movement of molecules through the paracellular space (gate function) and also maintains the polarization of apical and basolateral membrane domains by restricting the movement of lipids and membrane proteins within the plane of the membrane (fence function).

Since the identification and characterization of the membrane-associated guanylate kinase (MAGUK) protein ZO-1 (Stevenson et al., 1986), other TJ-associated proteins have been discovered, now totaling at least 15 peripheral and 3 integral membrane proteins including the multiple members of the claudin family (Morita et al., 1999). However, our understanding of the functions of these proteins, particularly those peripherally associated with the TJ membrane, is minimal. As a first step towards this understanding, determining how junctional proteins interact will help decipher TJ physiology at the molecular level. Two additional MAGUK family proteins, ZO-2 (Jesaitis and Goodenough, 1994; Beatch et al., 1996) and ZO-3 (Haskins et al., 1998) have been shown to interact directly with ZO-1 (Haskins et al., 1998; Wittchen et al., 1999) but not with each other (Haskins et al., 1998). ZO-1/ZO-2 and ZO-1/ZO-3 likely exist as two distinct heterodimers in vivo and not as a trimeric complex as previously thought (Wittchen et al., 1999). All three ZO proteins interact directly with the carboxy-terminal 150 amino acids of occludin (Furuse et al., 1994; Haskins et al., 1998; Wittchen et al., 1999) and claudin 1–8 (Itoh et al., 1999a). ZO-1, ZO-2, and ZO-3 also bind actin filaments (Itoh et al., 1997; Fanning et al., 1998; Wittchen et al., 1999), providing multiple linkage sites to the actin cytoskeleton. Furthermore, ZO-1, ZO-2, and ZO-3 all interact with another TJ plaque protein, cingulin (Cordenonsi et al., 1999), and ZO-1 can associate with the Ras-effector molecule AF-6 (Yamamoto et al., 1997) and the integral membrane protein JAM (Bazzoni et al., 2000).

Address correspondence to Dr. Bruce R. Stevenson, Department of Cell Biology, University of Alberta, Med. Sci. 5-19, Edmonton, Alberta, Canada T6G 2H7. Tel.: (780) 492-1841; Fax: (780) 492-0450; E-mail: bruce.stevenson@ualberta.ca

[1]*Abbreviations used in this paper:* AJ, adherens junction; cD, cytochalasin D; CZO-3, carboxy-terminal half of ZO-3; FLZO-3, full-length ZO-3; GUK, guanylate kinase; MAGUK, membrane-associated guanylate kinase; NZO-3, amino-terminal half of ZO-3; PDZ, PSD95/dlg/ZO-1; SH3, Src homology 3; TER, transepithelial resistance; TJ, tight junction; TX-100, Triton X-100; VSVG, vesicular stomatitis virus glycoprotein.

ZO-1, ZO-2, and ZO-3 contain a conserved series of well-known protein–protein interaction motifs. All three proteins have three amino-terminal PSD95/dlg/ZO-1 (PDZ) domains, followed by a Src homology 3 (SH3) domain and a guanylate kinase (GUK) domain. The carboxy-terminal portion of ZO-1 and ZO-2 consists of a proline-rich region; however, in ZO-3 this proline-rich region is located in the amino-terminal half of the protein between PDZ2 and PDZ3. The specific domains responsible for the various binding interactions of ZO-1, ZO-2, and ZO-3 have, in part been defined. ZO-1 and ZO-2 form a complex through reciprocal interactions between their PDZ2 domains (Fanning et al., 1998; Itoh et al., 1999b), and ZO-3 likely interacts with ZO-1 in the same manner (Itoh et al., 1999a). ZO-1 interaction with occludin likely occurs through the GUK domain, and actin binding via a region that encompasses the proline-rich domain of ZO-1 (Fanning et al., 1998). ZO-1, ZO-2, and ZO-3 binding to the carboxy-terminal YV sequence of claudin 1–8 requires the first PDZ domain of each protein (Itoh et al., 1999a). Finally, the amino-terminal region of ZO-1 and ZO-2 binds to α-catenin, and ZO-1 and ZO-2 are components of the adherens junction (AJ) in certain nonepithelial cells (Itoh et al., 1997, 1999b). No further information on individual domain binding characteristics or overall protein function(s) is available for ZO-3.

One current model for TJ assembly involves the coordinate assembly of the AJ and TJ. This model proposes that the first step in de novo junction formation involves E-cadherin–mediated cell adhesion (Gumbiner et al., 1988), followed by ZO-1 recruitment to the lateral surface of the cell via a transient interaction with the α-/β-catenin complex (Rajasekaran et al., 1996). Indeed, it was subsequently found that ZO-1 binds α-catenin in vitro (Itoh et al., 1997), providing the means by which ZO-1 is associated with the catenin complex during this early stage in junction formation. As epithelial polarization proceeds, ZO-1 is sorted out of the AJ and forms part of a separate TJ complex (Ando-Akatsuka et al., 1999). In vitro binding experiments have shown that ZO-2 can also bind α-catenin (Itoh et al., 1999b), indicating the possibility that ZO-2 may follow a similar path during initial stages of junctional complex assembly, either directly via interaction with α-catenin or indirectly via its association with ZO-1 (Wittchen et al., 1999). Recent data suggest that this hierarchy of junctional complex assembly is not absolute. Troxell et al. (2000) have shown that TJ assembly was extensive in MDCK cells expressing a mutant E-cadherin protein lacking the extracellular domain required for cell–cell adhesion, suggesting the possibility that TJs can assemble in the absence of an initial E-cadherin–mediated cell adhesion event.

Here we pursue the role of ZO-3 in epithelial cell physiology by expressing mutant ZO-3 constructs in MDCK cells. Through studies on TJ assembly and the domains responsible for protein–protein interactions, we have demonstrated that exogenous expression of the PDZ domain-containing, amino-terminal half of ZO-3 perturbs both TJ and AJ assembly. Moreover, such expression also affects actin dynamics and the biochemical properties of at least one adherens junction protein. Through in vitro binding assays we show that this amino-terminal half of ZO-3 preferentially binds ZO-1 and actin filaments. These studies provide the first functional information on ZO-3 and help to define how the molecular constituents of the junctional complex may interact and assemble in epithelial cells.

Materials and Methods

Plasmid Construction and MDCK Transfections

The ZO-3 constructs used in this study are shown in Fig. 1. A vesicular stomatitis virus glycoprotein (VSVG) epitope-tagged version of full-length ZO-3 (FLZO-3) in the expression vector pBK-CMV used for transfection of MDCK cells has been described (Haskins et al., 1998). The stable cell line MDCK/FLZO-3 was generated by transfection using Lipofectin (GIBCO BRL) and G418 selection as described (Haskins et al., 1998). A construct composed of the amino-terminal half of ZO-3 (NZO-3) contains the three PDZ domains, arginine-rich region, and proline-rich domain (amino acids 1–454). For stable transfection in MDCK cells, this construct was subcloned into pBK-CMV with a VSVG epitope tag inserted at the carboxy terminus. NZO-3 was also subcloned into the pFastBac HT vector series of the Baculovirus eukaryotic expression system (GIBCO BRL) to generate a 6-histidine–tagged protein used for in vitro binding experiments. A construct composed of the entire carboxy-terminal half of ZO-3 (CZO-3) containing the SH3 and GUK domains, followed by the acidic region (amino acids 455–899) was subcloned into pBK-CMV with a VSVG-epitope tag at the carboxy terminus and stably transfected into MDCK cells. CZO-3 was also inserted into the pFastBac HT vector series to generate a 6-histidine–tagged recombinant protein for binding analyses. For each stable cell transfection, multiple clones were selected and analyzed for expression of constructs by immunofluorescence and immunoblotting.

Calcium Switch and Cytochalasin D Treatment

For transepithelial resistance (TER) measurements and immunohistochemistry, untransfected or transfected MDCK cells grown as previously described (Howarth et al., 1992) were plated on Transwell polycarbonate membrane filter inserts (0.4 μm pore size; Costar Corp.) coated with rat tail collagen at a cell density of 3×10^5 cells/cm^2. Filters were fed every day. Calcium switch experiments were performed with minor modifications of previously published methods (Cereijido et al., 1978; Gumbiner and Simons, 1986). In brief, cells were trypsinized and replated on filters in DME containing 1.8 mM calcium for 2–3 h to allow attachment. Filters were then rinsed 2× with PBS without added calcium (PBS−) before switching to low calcium (5 μM) DME overnight (~15 h) to allow disassembly of the junctional complex. Cells were then switched back to 1.8 mM calcium-containing media at $t = 0$, and junctional reassembly was followed for various times. Control cells used for determination of steady-state levels of NZO-3 were trypsinized, replated in normal calcium media, and incubated for ~65 h.

Cytochalasin D (cD) (4 μg/ml) in Hepes-buffered saline plus glucose (HBSG; 10 mM Hepes, pH 7.4, 5.4 mM KCl, 137 mM NaCl, 1.3 mM $CaCl_2$, 0.5 mM $MgCl_2$, 5.6 mM glucose), was added to filter-grown monolayers for 60 min and then was washed out by rinsing filters 3× with HBSG. Cells were then incubated in HBSG without cD for another 2 h.

Transepithelial Resistance Measurements

TER was measured with a Millicell-ERS apparatus (Millipore) in HBSG as previously described (Stevenson and Begg, 1994). In the results depicted in Fig. 3 (A and B), duplicate filters from each cell line were measured for each time point, and the experiment was performed at least twice. Data from at least two experiments ($n > 4$ filters) are presented as mean ± SEM. Data from single clones of parental, MDCK/NZO-3, MDCK/CZO-3, and MDCK/FLZO-3 cells are shown. Two additional, independently selected MDCK/NZO-3 cell lines were tested in both the calcium switch and cD experiments and showed results essentially identical to the first MDCK/NZO-3 cell line (data not shown). For calcium switch experiments (see Fig. 3 A), TER is plotted in ohm × cm^2. For cD experiments (see Fig. 3 B), TER is expressed as a percentage normalized to $t = 0$. The steady-state TER of all cell lines examined was 50–60 ohm × cm^2.

Antibodies

The following antibodies were used: rat anti–ZO-1 mAb R40.76 (Anderson et al., 1988), rabbit anti–ZO-2 polyclonal Ab R9989 (Jesaitis and Goodenough, 1994), rabbit anti-VSVG (a gift from Dr. Carolyn Machamer, Johns Hopkins University, Baltimore, MD), rabbit anti-occludin

(Wong and Gumbiner, 1997; a gift from Drs. Alpha Yap and Barry Gumbiner, Memorial Sloan-Kettering Cancer Center, New York, NY), mouse anti–E-cadherin mAb 3G8, (a gift from Dr. Warren Gallin, University of Alberta, Edmonton, Canada), and rabbit anti–β-catenin (Sigma-Aldrich; No. C2206). For detection of ZO-3 constructs, the following antibodies were used: guinea pig anti–ZO-3 (Haskins et al., 1998) and mouse anti–ZO-3 mAB3260 (Chemicon International, Inc.), which both recognize an epitope in the amino terminus of ZO-3 and were used to detect full-length ZO-3 and NZO-3; rabbit anti–ZO-3 polyclonal AB3220 (Chemicon International, Inc.) recognizes an epitope in the extreme carboxy terminus of ZO-3 and was used to detect CZO-3. HRP-conjugated goat anti–rabbit and HRP-conjugated goat anti–mouse (Bio-Rad Laboratories), HRP-conjugated goat anti–guinea pig and HRP-conjugated anti–rat (Jackson ImmunoResearch Laboratories) were used as secondary antibodies for immunoblots. Rhodamine-conjugated donkey anti–rabbit, rhodamine-conjugated donkey anti–guinea pig, rhodamine-conjugated goat anti–rat, rhodamine-conjugated goat anti–mouse, FITC-conjugated goat anti–rat, and Texas red–conjugated goat anti–mouse (Jackson ImmunoResearch Laboratories) were used as secondary antibodies for indirect immunofluorescence.

Immunohistochemistry

For immunofluorescence staining with anti-VSVG, cells grown on collagen-coated coverslips were fixed with 5% acetic acid in ethanol for 5 min at −20°C and permeabilized with 0.2% Triton X-100 (TX-100) in TBS plus 1.8 mM calcium (TBS+) for 4 min at room temperature. For all other staining, cells grown on filters were fixed with 2.5% paraformaldehyde in TBS and permeabilized with 0.2% TX-100. Rhodamine-conjugated phalloidin (Sigma-Aldrich) was used to stain F-actin. Coverslips and filters were viewed on a Zeiss Axioskop (Carl Zeiss, Inc.).

Protein Expression Analysis and TX-100 Extraction

Parental or MDCK/NZO-3 cells grown on 35-mm tissue culture dishes were subjected to a calcium switch, and total lysates were made from cells 6, 12, 24, and 48 h after the re-addition of calcium. The steady-state level of NZO-3 was assessed on control cells not subjected to calcium switch that were maintained in normal calcium media for ~65 h. Monolayers were rinsed 2× with ice-cold TBS+ and scraped up into 1 ml ice-cold TBS+ plus protease inhibitor cocktail (1 μg/ml aprotinin, 1 μg/ml chymostatin, 1 μg/ml leupeptin, 1 μg/ml pepstatin, and 1 mM Pefabloc SC; Boehringer). Scraped cells were then harvested by centrifugation at 6,500 rpm for 5 min at 4°C. Cell pellets were resuspended in hot SDS lysis buffer (10 mM Tris, pH 7.8, 1% SDS) plus protease inhibitors and boiled for 5 min, shearing with a narrow bore pipette tip. Protein concentration was determined by BCA protein assay (Pierce Chemical Co.) and 20 μg total protein was loaded per lane on SDS-PAGE. For immunoblots, gels were electrophoretically transferred to nitrocellulose, immunoblotted with corresponding antibodies, and proteins detected via ECL (Amersham Pharmacia Biotech).

For separation of TX-100–soluble and –insoluble β-catenin, parental and MDCK/NZO-3 cells subjected to a calcium switch were extracted with CSK buffer (10 mM Pipes, pH 6.8, 50 mM NaCl, 300 mM sucrose, 0.5% TX-100 plus 0.1 mg/ml DNAse, 0.1 mg RNAse, and protease inhibitor cocktail; Troxell et al., 2000). In brief, cell monolayers grown on 35-mm dishes were rinsed 2× with ice-cold TBS+ and then extracted for 10 min on ice with 1.5 ml CSK buffer. Insoluble material was scraped from the dish, and the extracts were centrifuged 10 min at 13,000 rpm at 4°C. Supernatants contain the detergent-soluble pool of β-catenin. Pellets containing detergent-insoluble material were resuspended in 1.5 ml hot SDS lysis buffer and boiled for 10 min. Protein concentration in each fraction was determined by BCA protein assay, and samples were loaded for SDS-PAGE and immunoblot analysis as above.

Recombinant Protein Expression and In Vitro Binding Studies

Recombinant 6-histidine–tagged NZO-3 and CZO-3 were expressed in Sf9 insect cells using a Baculovirus eukaryotic expression system (GIBCO BRL) and purified according to previously published methods (Haskins et al., 1998; Wittchen et al., 1999). Empty expression vector encoding the 6-histidine tag plus 36 nonspecific amino acids served as the negative control. Equal amounts of purified NZO-3 and CZO-3 were used in the binding experiments. [^{35}S]Methionine-labeled in vitro–transcribed/translated human ZO-1 was prepared as described (Haskins et al., 1998; Wittchen et al., 1999). Expression of GST-occludin encoding the carboxy-terminal 150 amino acids of the cytoplasmic tail of chicken occludin (Furuse et al., 1993) was described previously (Haskins et al., 1998; Wittchen et al., 1999). GST–N-cingulin cDNA encoding the amino-terminal head region (amino acids 1–378) of *Xenopus* cingulin in pGEX-4T1 (a gift from Dr. Sandra Citi, University of Geneva, Geneva, Switzerland) was expressed according to published methods (Cordenonsi et al., 1999).

The binding of NZO-3 and CZO-3 to actin, ZO-1, and occludin was performed as previously described (Wittchen et al., 1999). Cingulin binding experiments used a modification of the methods of Cordenonsi et al. (1999). In brief, GST–N-cingulin or GST alone was immobilized on glutathione-Sepharose 4B beads, and equal amounts of purified NZO-3 or CZO-3 were added. Binding buffer comprised of PBS plus 1% TX-100 and protease inhibitors. Binding was allowed to proceed overnight at 4°C, followed by washing with the same buffer, and eluting bound protein by boiling the beads in gel sample buffer. NZO-3 and CZO-3 binding was detected by immunoblot, and in the case of occludin and cingulin binding experiments, the amount of bound NZO-3 and CZO-3 was compared by Coomassie blue staining of the bound fraction.

Results

The Effect of Truncated ZO-3 Constructs on Tight Junction Physiology

We first determined which region of ZO-3 encodes the information for targeting the protein to the TJ. MDCK cells were stably transfected with the VSVG-tagged FLZO-3, NZO-3, and CZO-3 constructs (Fig. 1). Subcellular localization of the constructs was detected by indirect immunofluorescence using anti-VSVG antibodies and costaining for ZO-1 as a marker for the TJ. FLZO-3 correctly targets to cell borders, colocalizing with the TJ marker ZO-1 (data not shown). The NZO-3 construct also colocalizes with endogenous ZO-1 at cell borders (Fig. 2); furthermore, its localization was also indistinguishable from endogenous ZO-1 as assayed by 0.2 μm Z-section confocal microscopy (data not shown). The nuclear staining visible with the anti-VSVG staining is nonspecific as the same staining pattern is seen in untransfected parental MDCK cells (see Fig. 5 A). Fig. 2 also shows that when expressed in MDCK cells, CZO-3 is absent from cell borders and is instead diffusely distributed in the cytoplasm. Expression of the CZO-3 construct in these cells was confirmed by immunoblot (data not shown). Combined, these data indicate that the information necessary for proper targeting of ZO-3 to the TJ is contained within the amino-terminal half of the protein.

We next examined the effect of exogenous expression of these constructs on TJ formation using two experimental paradigms. The first approach is based on the observation

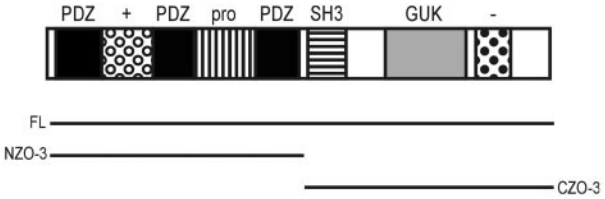

Figure 1. Schematic diagram of the ZO-3 constructs used in this study. Full-length ZO-3 (FLZO-3) contains three PDZ domains, an arginine-rich basic region (+), a proline-rich region (pro), an SH3 domain, a GUK domain, and an acidic region (−). NZO-3 comprises the amino-terminal half of ZO-3 and contains the three PDZ domains, basic region and proline-rich region. The CZO-3 construct corresponds to the carboxy-terminal half of the molecule and contains the SH3, GUK, and acidic domains. The constructs used for generating stably transfected MDCK cells have a VSVG epitope tag at their carboxy terminus.

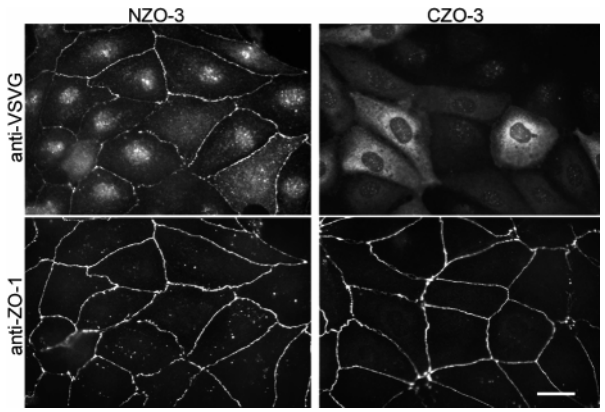

Figure 2. The NZO-3 construct correctly targets to the TJ; the CZO-3 does not. MDCK cells were stably transfected with VSVG-tagged NZO-3 (MDCK/NZO-3) or CZO-3 (MDCK/CZO-3) constructs. Transfected cells were costained with anti–ZO-1 and anti-VSVG antibodies to mark the TJ and localize the constructs by indirect immunofluorescence. NZO-3 precisely colocalizes with ZO-1 at cell borders, with additional staining visible in the cytoplasm. CZO-3 is found mainly in the cytoplasm and is absent from cell borders. The nuclear staining in the MDCK/NZO-3 cells stained with anti-VSVG is nonspecific (see Fig. 5). Bar, 15 μm.

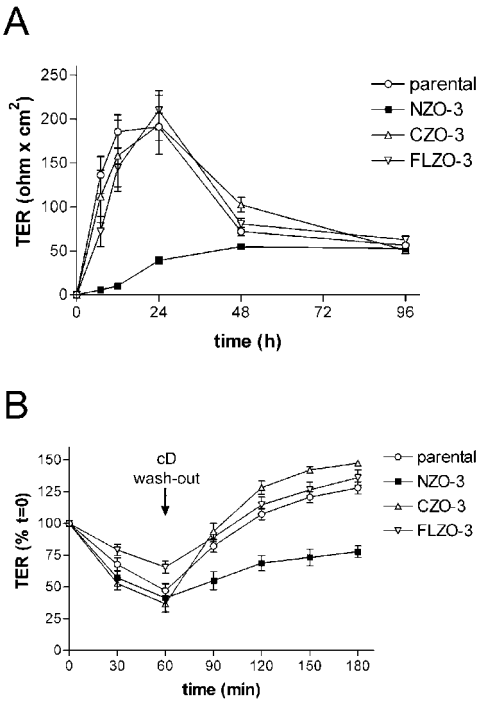

Figure 3. Expression of NZO-3 delays TJ formation. (A) NZO-3 expression in MDCK cells subjected to a calcium switch delays re-establishment of TER. Filter-grown confluent monolayers of untransfected parental cells or MDCK cell lines stably expressing NZO-3, CZO-3, or FLZO-3 were incubated in calcium-free media for ~15 h to disrupt intercellular junctions and then switched to media containing 1.8 mM calcium at $t = 0$ to induce synchronous assembly of intercellular junctions. TER was measured over 96 h after calcium switch. CZO-3 and FLZO-3 expressing cell lines show TER recovery dynamics similar to parental cells. NZO-3–expressing cells display a delay in TER recovery, but reach the same TER as the other cell lines by 48–96 h. (B) Expression of NZO-3 delays TER recovery in MDCK cells after cD treatment. cD was added to filter-grown confluent monolayers at $t = 0$ and then washed out after 60 min. TER measurements were taken every 30 min to monitor TJ breakdown and reformation. TER for each cell line is expressed as percentages of the values at $t = 0$. After 60 min of cD treatment, all cell lines exhibit a significant drop in TER. After cD washout, MDCK/CZO-3, MDCK/FLZO-3 and parental cells recover TER to values greater than $t = 0$, whereas MDCK/NZO-3 cells do not fully recover TER in the duration of the experiment.

that AJs and TJs are disrupted if epithelial cells are grown in medium containing subphysiological calcium concentration (5 μM). Subsequent restoration of physiological levels of calcium (1.8 mM) results in the synchronous de novo assembly of both junction types (Cereijido et al., 1978; Gumbiner and Simons, 1986). Filter-grown monolayers of parental, NZO-3, CZO-3, or FLZO-3–expressing MDCK cells were grown overnight in low calcium media. Physiological concentration of calcium was added back at $t = 0$, and TJ assembly was monitored by measuring TER over a 48-h time period. As shown in Fig. 3 A, parental MDCK cells undergo an initial rapid increase in TER to over 175 ohm × cm^2 by 12 h. Resistance peaked at 12–24 h, before declining and leveling off to ~50 ohm × cm^2 by 96 h. Cell lines expressing the CZO-3 and FLZO-3 constructs followed a similar trend, plateauing at the same steady-state level as parental cells. In contrast, NZO-3–expressing cells exhibited delayed TER development, with no initial overshoot typical of the other cell lines. However, regardless of the delay, NZO-3–expressing cells reached a steady-state TER similar to that of the other cell lines by 48–96 h. The TER of all cells at 96 h is similar to that of untreated cells (data not shown).

We corroborated the results obtained in the calcium switch experiments by determining the effect of ZO-3 construct expression on TJ reformation in MDCK cells treated with the actin-disrupting drug cD. In cells treated with cD, the apical actin cytoskeletal ring associated with the junctional complex is disrupted into large punctate aggregates that colocalize with similarly disrupted TJ proteins ZO-1, ZO-2, ZO-3, and occludin (Stevenson and Begg, 1994; Wittchen et al., 1999). The cD-treated cells also show a sharp drop in TER, indicating a loss of functional TJs. It was shown that this effect is reversible, and upon washout of cD, TJs reassemble synchronously (Madara et al., 1986; Stevenson and Begg, 1994). We treated our MDCK cell lines with cD for 60 min, and the drug was then washed out (Fig. 3 B). Upon cD treatment all cell lines exhibited an immediate and substantial decrease in TER. After cD washout, parental, FLZO-3–, and CZO-3–expressing cells recovered TER values equal to or greater than $t = 0$ values within 1 h. However, NZO-3–expressing cells showed a delayed TER recovery from cD treatment and failed to reach $t = 0$ levels for the duration of the experiment. This result is in agreement with the calcium switch experiment (Fig. 3 A) and demonstrates that MDCK cells expressing the NZO-3 construct display an impaired ability to assemble functional TJs.

Junctional Protein Localization

The physiological data suggesting impaired TJ-forming ability in NZO-3–expressing cells prompted us to assess the localization of proteins associated with both TJs and AJs in the calcium switch experimental system. Parental and MDCK/NZO-3 cells grown on filters were subjected

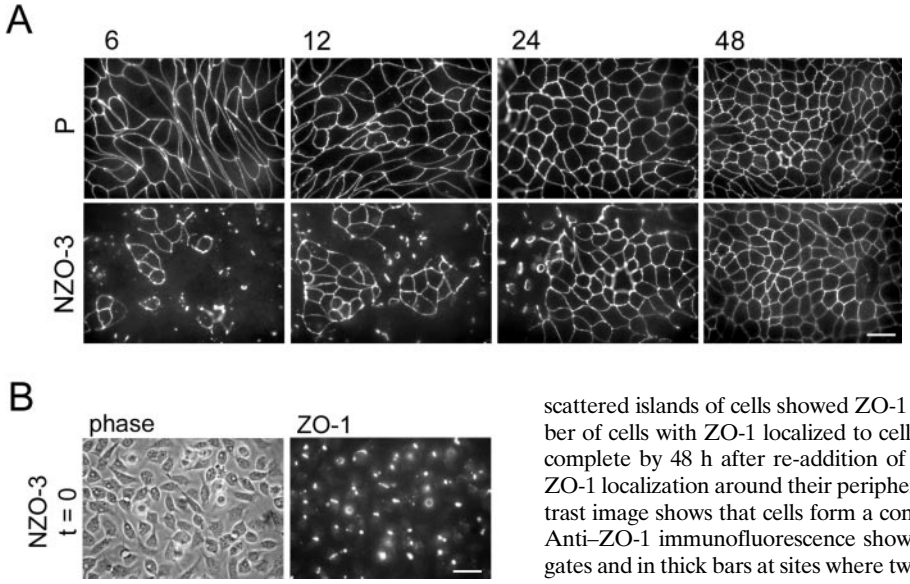

Figure 4. NZO-3 expression alters the distribution of ZO-1 during the early stages of TJ assembly. (A) Parental MDCK (P) and MDCK/NZO-3 (NZO-3) cells were subjected to a calcium switch, and the localization of ZO-1 at 6, 12, 24, and 48 h after the re-addition of calcium was determined by immunofluorescence with anti–ZO-1 antibody. In parental cells, ZO-1 is completely localized to cell borders after 6 h in calcium-containing media. Over 48 h the cells become more tightly packed and uniform in size. In NZO-3 expressing cells, only scattered islands of cells showed ZO-1 localization at cell borders by 6 h. The number of cells with ZO-1 localized to cell–cell contact sites increases over time and is complete by 48 h after re-addition of calcium. (B) No MDCK/NZO-3 cells show ZO-1 localization around their peripheries at $t = 0$ in the calcium switch. Phase-contrast image shows that cells form a confluent monolayer at $t = 0$ of calcium switch. Anti–ZO-1 immunofluorescence shows ZO-1 staining in large intracellular aggregates and in thick bars at sites where two cells make contact. Bars: (A and B) 30 μm.

to a calcium switch and protein localization was determined 6, 12, 24, and 48 h after re-addition of calcium. As shown in Fig. 4 A, ZO-1 is localized at cell–cell contacts within 6 h after re-addition of calcium. In the 12–48-h time period, the parental cells develop the cobblestone uniformity of shape and size that is typical of an MDCK epithelial cell monolayer at steady-state. The appearance of ZO-1 at cellular contacts 6 h after re-addition of calcium correlates well with the rapid increase in TER observed in the parental cells (Fig. 3 A). In contrast, cells expressing NZO-3 showed a significant delay in ZO-1 recruitment to cell borders after re-addition of calcium (Fig. 4 A). At 6 h, only small, isolated clusters of cells showed ZO-1 staining at cell borders. Over time the areas of cell monolayer that show ZO-1 localization at cell–cell contacts increase in size. At 6, 12, and 24 h when ZO-1 is not yet fully localized to cell borders, ZO-1 also localizes to large intracellular aggregates and linear planes of contact between neighboring cells. Complete localization of ZO-1 at the junctional membrane in NZO-3–expressing cells did not occur until 48 h after re-addition of calcium. ZO-1 localization in both cell types at 48 h is indistinguishable from untreated, steady-state cells (data not shown). Both parental and MDCK/NZO-3 cells displayed no detectable differences in expression levels of ZO-1 (or any other junctional protein examined; see Fig. 9 immunoblot) at 6, 12, 24, and 48 h. The delayed targeting of the TJ protein ZO-1 in MDCK/NZO-3 cells correlates with the delay in TER recovery after calcium switch (Fig. 3 A). The localization of the TJ proteins ZO-2, endogenous ZO-3, and the integral membrane protein occludin was identical to that of ZO-1 in the MDCK/NZO-3 cells (data not shown).

To rule out the possibility that the isolated islands of MDCK/NZO-3 cells showing ZO-1 staining encircling cell peripheries at 6 h arose from cell clusters that did not disassemble their TJs during incubation in low calcium, and to demonstrate that the recruitment of ZO-1 to cell peripheries occurred de novo, we looked at ZO-1 localization in MDCK/NZO-3 cells before the re-addition of calcium ($t = 0$). As viewed by phase-contrast microscopy, cells plated at an identical density on glass coverslips show a confluent distribution at $t = 0$, although the cells are somewhat retracted from each other due to the dissociation of adherens and TJs in low calcium (Fig. 4 B). ZO-1 staining is completely disrupted, and is present only in large intracellular aggregates and thick, linear planes of contact between neighboring cells. No cells show ZO-1 staining encircling their peripheries at $t = 0$. Thus, ZO-1 (and ZO-2, endogenous ZO-3, and occludin; data not shown) is recruited from an intracellular location to cell–cell contacts upon re-addition of calcium, and this recruitment process is delayed in NZO-3–expressing MDCK cells.

The disrupted localization of TJ proteins during junctional assembly after calcium switch in cells expressing NZO-3 indicates that this construct interferes with the formation of the complex of proteins found at the TJ. We therefore examined the localization of the construct itself during this process. The anti-VSVG antibody only weakly recognizes its epitope on NZO-3 in immunofluorescence and was not visible in filter-grown cells. Hence, MDCK/NZO-3 cells grown on coverslips and subjected to a calcium switch were costained with the anti–ZO-1 and anti-VSVG (NZO-3) antibodies. Parental MDCK cells stained with anti-VSVG serve as a negative control and show that this antibody exhibits nonspecific nuclear staining in untransfected cells (Fig. 5 A). At the earliest time points (6, 12, and 24 h), the NZO-3 construct appears at only those cell borders that also show ZO-1 localization. MDCK/NZO-3 cells stained with anti-VSVG antibody also exhibit a faint, granular cytoplasmic staining above background. NZO-3 staining is only faintly visible at 48 h, likely due to the lower levels of construct expression at this time point (see Fig. 9 immunoblot). In areas where NZO-3 is visible, it was colocalized with ZO-1 at all cell–cell contacts. Interestingly, NZO-3 was absent from the intracellular aggregates and linear planes of ZO-1 staining observed at early time points, and was only colocalized with ZO-1 at points of cell–cell contact formed by mature TJs (Fig. 5 B).

The actin cytoskeleton is an important structural and a functional element of the TJ (Hirokawa and Tilney, 1982; Madara, 1987). Actin filaments have been shown to interact directly with multiple TJ proteins (Itoh et al., 1997;

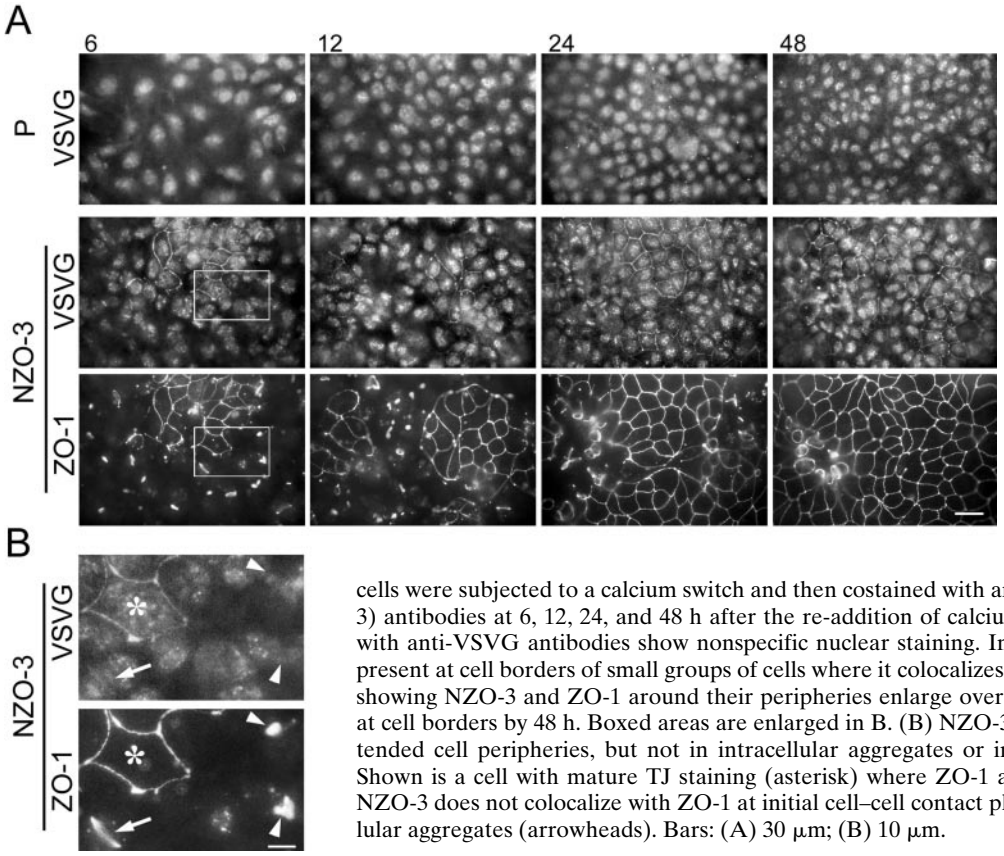

Figure 5. NZO-3 colocalizes with ZO-1 around cell borders during TJ assembly after calcium switch. (A) Parental MDCK (P) and MDCK/NZO-3 (NZO-3) cells were subjected to a calcium switch and then costained with anti–ZO-1 and anti-VSVG (NZO-3) antibodies at 6, 12, 24, and 48 h after the re-addition of calcium. Parental MDCK cells stained with anti-VSVG antibodies show nonspecific nuclear staining. In MDCK/NZO-3 cells, NZO-3 is present at cell borders of small groups of cells where it colocalizes with ZO-1. These groups of cells showing NZO-3 and ZO-1 around their peripheries enlarge over time, with complete localization at cell borders by 48 h. Boxed areas are enlarged in B. (B) NZO-3 colocalizes with ZO-1 along extended cell peripheries, but not in intracellular aggregates or initial planes of cell–cell contact. Shown is a cell with mature TJ staining (asterisk) where ZO-1 and NZO-3 colocalize. However, NZO-3 does not colocalize with ZO-1 at initial cell–cell contact planes (arrow) or in large intracellular aggregates (arrowheads). Bars: (A) 30 μm; (B) 10 μm.

Fanning et al., 1998; Wittchen et al., 1999). Disruption of the actin cytoskeleton is associated with impaired barrier function of the TJ (Madara et al., 1986; Madara and Pappenheimer, 1987; Stevenson and Begg, 1994), whereas the fence function appears to be unaffected (Takakuwa et al., 2000). Actin localization during TJ assembly in the calcium switch system was studied by rhodamine-phalloidin staining of actin filaments (Fig. 6). In parental MDCK cells, actin recruitment to a ring-like structure at the apical aspect of the lateral cell surface occurs rapidly after re-addition of calcium; as early as 6 h all parental cells show a circumferential actin ring. This ring thickens and condenses as the cells become more tightly packed and uniform in size in the 12–48-h time period. However, exogenous expression of NZO-3 delays recruitment of actin to the apical ring in a manner similar to that observed with ZO-1. Development of an apical actin ring at points of cell–cell contact in MDCK/NZO-3 cells occurred only in isolated patches of cells at 6 h, with the final localization not complete until 48 h. In addition, at the earlier time points (6, 12, and 24 h), actin also localized to large aggregates in cells which show underdeveloped actin rings. The delayed association of actin filaments with the junctional complex in MDCK/NZO-3 cells is likely a factor in the delayed TJ barrier formation in these cells.

As the prevalent model of TJ formation involves coordinated assembly with the AJ, we were interested to determine if E-cadherin was delayed in its movement to the junctional complex in MDCK/NZO-3 cells in a calcium switch. In parental cells, E-cadherin appears at all cell–cell contacts 6 h after re-addition of calcium (Fig. 7). This time course of E-cadherin recruitment to the AJ mirrors that of TJ assembly and recruitment of ZO-1 to the TJ (Fig. 4 A). Similar to ZO-1, E-cadherin localization during the calcium switch was also delayed in NZO-3–expressing cells (Fig. 7). At 6 h, E-cadherin is localized to cell–cell contacts in small, isolated clusters of cells; these cell clusters also show ZO-1 localization to the junctional complex. An increasing number of cells show junctional E-cadherin staining at 12 and 24 h, but it is not until 48 h after calcium re-addition that E-cadherin is completely recruited to all cell borders in MDCK/NZO-3 cells. In addition, we identified cells where junctional recruitment of E-cadherin precedes that of ZO-1. The disruption of E-cadherin localization in MDCK/NZO-3 cells after calcium switch indicates that adherens and TJs are both affected by exogenous expression of the NZO-3 construct. We corroborated our E-cadherin findings by assessing the localization of β-catenin, an AJ protein peripherally associated with the membrane (Fig. 8). In parental cells, β-catenin appears at cell–cell contacts 6 h after calcium re-addition in a manner identical to the localization of E-cadherin after calcium switch (data not shown). However, in a distribution similar to E-cadherin and ZO-1, β-catenin recruitment to the lateral cell surface during junctional complex assembly was delayed in MDCK/NZO-3 cells.

Protein Biochemistry

In addition to the altered localization of junctional complex proteins and disruption of the actin cytoskeleton, it is possible that the perturbation of junctional assembly in NZO-3–expressing cells is also due to changes in the expression levels of component proteins. Equivalent protein loadings of whole cell lysates harvested from parental and MDCK/NZO-3 cells at 6, 12, 24, and 48 h after re-

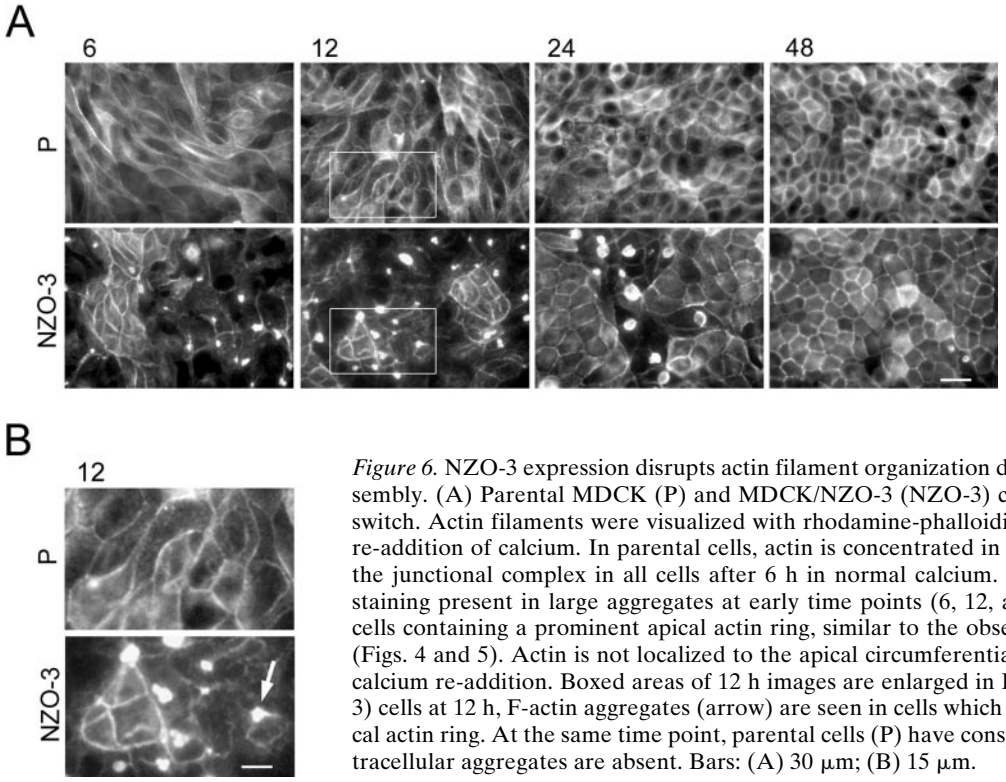

Figure 6. NZO-3 expression disrupts actin filament organization during early stages of junction assembly. (A) Parental MDCK (P) and MDCK/NZO-3 (NZO-3) cells were subjected to a calcium switch. Actin filaments were visualized with rhodamine-phalloidin at 6, 12, 24, and 48 h after the re-addition of calcium. In parental cells, actin is concentrated in an apical circumferential ring at the junctional complex in all cells after 6 h in normal calcium. MDCK/NZO-3 cells show actin staining present in large aggregates at early time points (6, 12, and 24 h), with small clusters of cells containing a prominent apical actin ring, similar to the observations with ZO-1 and NZO-3 (Figs. 4 and 5). Actin is not localized to the apical circumferential ring in all cells until 48 h after calcium re-addition. Boxed areas of 12 h images are enlarged in B. (B) In MDCK/NZO-3 (NZO-3) cells at 12 h, F-actin aggregates (arrow) are seen in cells which have not fully developed an apical actin ring. At the same time point, parental cells (P) have conspicuous apical actin rings and intracellular aggregates are absent. Bars: (A) 30 μm; (B) 15 μm.

addition of calcium were immunoblotted for the NZO-3 construct, endogenous ZO-3, ZO-1, ZO-2, occludin, and E-cadherin (Fig. 9 A). As expected, no NZO-3 was detected in untransfected parental cells. NZO-3 expression in MDCK/NZO-3 cells increased in response to the calcium jump, with highest expression at 6 h. Construct expression then gradually decreased over time and returned to stable, steady-state levels. This decrease over time correlates well with recovery of TER and the normal localizations of junctional proteins over the same time period. The expression levels of all other proteins examined did not change over the course of the calcium switch in either parental or MDCK/NZO-3 cells. There was also no detectable difference in the expression levels between parental and MDCK/NZO-3 cells at any of the time points, indicating that the effects on junctional assembly caused by NZO-3 expression were not due to altered expression of other junctional proteins. We observed a shift in mobility of occludin in both parental and MDCK/NZO-3 cells to a higher molecular weight species over time, corresponding to an increase in phosphorylation of this protein as the TJ assembles, as previously described (Sakakibara et al., 1997).

In epithelial cells, β-catenin is found in two distinct pools: a TX-100–insoluble pool, which comprises the β-catenin molecules which are bound to E-cadherin and linked to the actin cytoskeleton via α-catenin, and a TX-100–soluble pool that represents the non–AJ-associated, cytoplasmic pool of free β-catenin (Fagotto et al., 1996; Funayama et al., 1995). Because these TX-100–soluble and –insoluble pools of β-catenin are functionally distinct, we examined the expression levels of β-catenin in equivalent protein loadings of TX-100–extracted parental and NZO-3–expressing cells. Fig. 9 B shows that at 12 and 24 h after re-addition of calcium there is more soluble β-catenin in MDCK/NZO-3 cells relative to parental cells. This difference is present but less pronounced at 48 h. Equivalent samples of the TX-100–insoluble fractions of parental and MDCK/NZO-3 cells show no difference in β-catenin levels. No differences were observed in the amount of α-catenin in the soluble or insoluble pools of TX-100–extracted parental or MDCK/NZO-3 cells (data not shown).

Protein Binding Analyses

We determined which of the known protein–protein interactions of ZO-3 could be mapped to the amino- and carboxy-terminal halves of the molecule. It has been previously shown that ZO-3 binds directly to actin filaments in vitro (Wittchen et al., 1999). In addition, ZO-3 also binds ZO-1, occludin, and the amino terminus of cingulin, but not to ZO-2 (Haskins et al., 1998; Cordenonsi et al., 1999). Fig. 10 A shows Coomassie-stained samples of the purified NZO-3 and CZO-3 proteins, demonstrating the equal amounts of these proteins used in subsequent binding experiments. As shown by actin cosedimentation assays in Fig. 10 B, substantial NZO-3 is found in the pellet in the presence of F-actin whereas a much smaller amount is visible in the pellet in the absence of actin, likely due to a low level of fusion protein aggregation. CZO-3 remained in the supernatant fraction in both the presence and absence of actin filaments. Therefore, the actin binding site(s) of ZO-3 reside in the amino terminus of the protein. To map the binding site(s) of ZO-1 on ZO-3, we performed a binding assay using ^{35}S-labeled in vitro–transcribed/translated human ZO-1 added to NZO-3 or CZO-3 affinity columns. As shown in Fig. 10 C, NZO-3 retains ZO-1, whereas CZO-3 and the negative control do not. This demonstrates that the amino-terminal half of ZO-3 is responsible for binding to ZO-1. This is consistent with previous studies

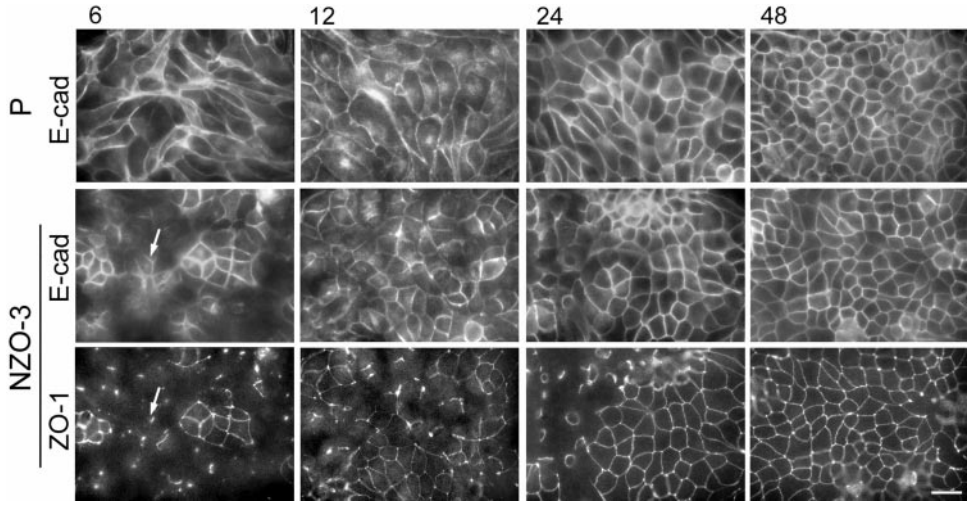

Figure 7. NZO-3 expression delays recruitment of E-cadherin to cell–cell contacts. Parental (P) and MDCK/NZO-3 (NZO-3) cells were subjected to a calcium switch, and E-cadherin and ZO-1 localization was monitored by costaining at 6, 12, 24, and 48 h after the re-addition of calcium. In parental cells, E-cadherin is localized to cell borders by 6 h. By 48 h, cell monolayers have an organized morphology. NZO-3–expressing cells costained with anti–ZO-1 and anti–E-cadherin antibodies show a delayed E-cadherin recruitment to cell borders. The clusters of cells that show E-cadherin localization at cell peripheries at early time points coincide with cells showing a similar distribution of ZO-1. Some cells (arrow) show E-cadherin at cell borders preceding ZO-1. E-cadherin staining at cell borders is complete by 24 h after the readdition of calcium, whereas ZO-1 staining at cell peripheries is not complete until 48 h. Bar, 30 μm.

showing that ZO-1 and ZO-2 bind each other via their second PDZ domains (Fanning et al., 1998; Itoh et al., 1999b). To define the occludin binding site on ZO-3, in vitro binding assays were performed using NZO-3 and CZO-3 added to affinity columns containing immobilized GST-occludin or GST alone, and bound proteins were detected by immunoblot (Fig. 10 D). Both NZO-3 and CZO-3 were specifically retained on the occludin column. Although the NZO-3 immunoblot reaction is stronger than that for CZO-3, the amounts of NZO-3 and CZO-3 bound to occludin appear approximately equivalent, as assayed by Coomassie blue staining of the bound fractions. This indicates that occludin binding domains of approximately equal affinity are found in both the amino- and carboxy-terminal halves of ZO-3. It has recently been reported that the amino-terminal head and to a lesser degree, the carboxy-terminal tail of cingulin bind to full-length ZO-3 in vitro (Cordenonsi et al., 1999). Here we determined which half of ZO-3 binds the amino-terminal portion of cingulin. Equivalent amounts of NZO-3 or CZO-3 were added to GST-cingulin or GST affinity columns. As shown in Fig. 10 E, both NZO-3 and CZO-3 are specifically retained by cingulin. Coomassie blue staining of the bound fractions revealed no significant difference between the amounts of NZO-3 or CZO-3 binding to cingulin, indicating that both halves of ZO-3 bind the head region of cingulin with approximately equal affinity. In summary, the binding studies shown in Fig. 10 reveal that while both halves of ZO-3 bind to occludin and cingulin equally well, F-actin and ZO-1 bind preferentially to NZO-3.

Discussion

In this study we have shown that exogenous expression of the amino-terminal half of ZO-3 delays assembly of both TJs and AJs. Analysis of protein expression showed that whereas the overall levels of the junctional proteins ZO-1, ZO-2, ZO-3, occludin, and E-cadherin remain constant during 48 h of junction assembly, NZO-3 expression increases in response to the calcium switch and then returns to stable, steady-state levels over the same time period. This return of NZO-3 expression to steady-state levels is concomitant with recovery of TER and localization of junctional proteins and actin to the membrane. The amount of β-catenin in the TX-100–soluble pool is also elevated in NZO-3 expressing cells. Finally, in vitro binding

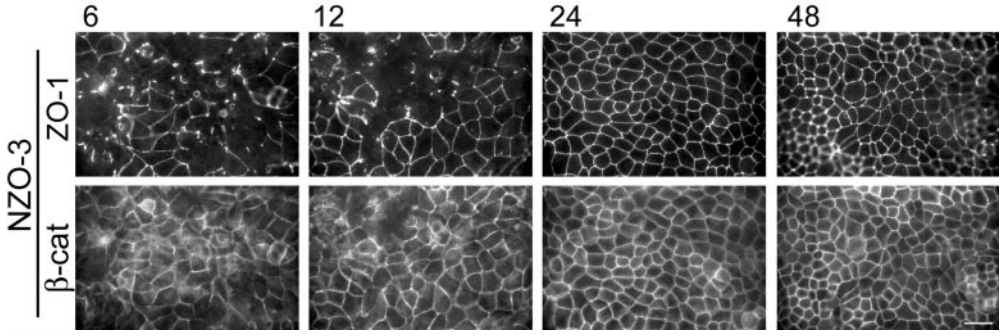

Figure 8. NZO-3 expression delays recruitment of β-catenin to cell–cell contacts. β-Catenin and ZO-1 localization in MDCK/NZO-3 cells was monitored at 6, 12, 24, and 48 h after the re-addition of calcium in a calcium switch experiment. NZO-3–expressing cells show a delayed β-catenin recruitment to intercellular junctions, which parallels the delay of E-cadherin recruitment (Fig. 7). The cells that show β-catenin localization at cell peripheries at early time points coincide with cells showing similar distribution of ZO-1, although many cells show β-catenin at cell borders preceding ZO-1. β-Catenin staining at cell borders is not complete until 24 h after the re-addition of calcium in MDCK/NZO-3 cells. Bar, 30 μm.

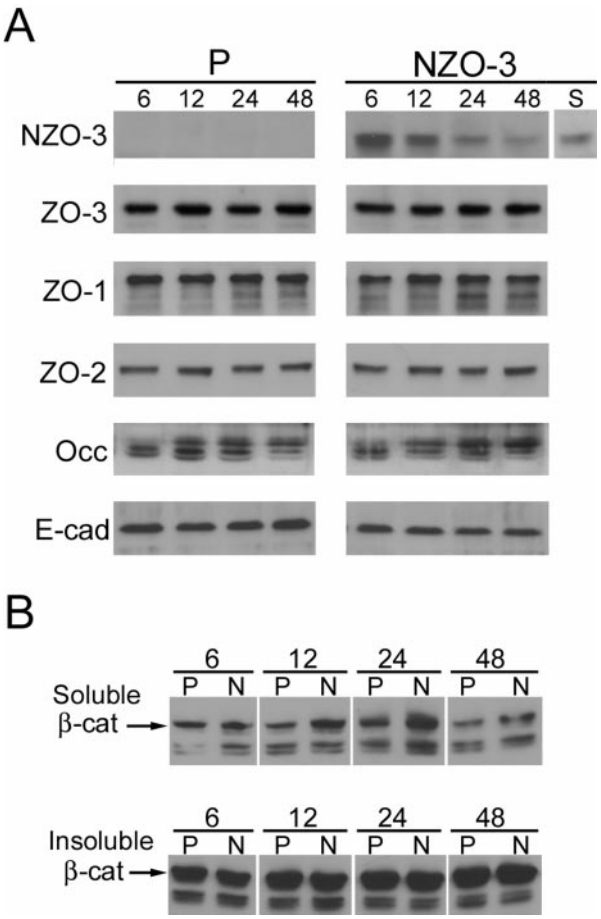

Figure 9. Expression levels of TJ and AJ proteins during a calcium switch experiment. (A) Equivalent protein loadings of whole cell lysates of parental (P) and MDCK/NZO-3 (NZO-3) cells were analyzed by immunoblot at 6, 12, 24, and 48 h after the re-addition of calcium. The monoclonal antibody against ZO-3 was used to detect both the NZO-3 construct and endogenous ZO-3; the proteins were distinguished by their difference in molecular mass. NZO-3 is not detected in parental cells. NZO-3 expression in MDCK/NZO-3 cells increases in response to the calcium switch and then over time returns to stable, steady-state levels (S). Endogenous ZO-3, ZO-1, ZO-2, occludin, and E-cadherin levels are unchanged during the course of the calcium switch experiment in both cell lines, and no significant differences in these protein levels are detected between parental and MDCK/NZO-3 cells at any time points. Occludin shows a shift to a higher molecular weight species in both cell lines over time. (B) MDCK/NZO-3 cells have more soluble β-catenin than parental cells. At indicated time points after a calcium switch, parental (P) and MDCK/NZO-3 (N) cells were extracted with CSK buffer (see Materials and Methods) to separate TX-100–soluble and –insoluble pools of β-catenin. Samples containing equal amounts of total cellular protein were analyzed for β-catenin expression by immunoblot. The amount of soluble β-catenin is greater in MDCK/NZO-3 cells than parental cells at 12 and 24 h, and to a lesser degree at 48 h after the re-addition of calcium. There is no detectable difference in the amount of insoluble β-catenin between parental and MDCK/NZO-3 cells.

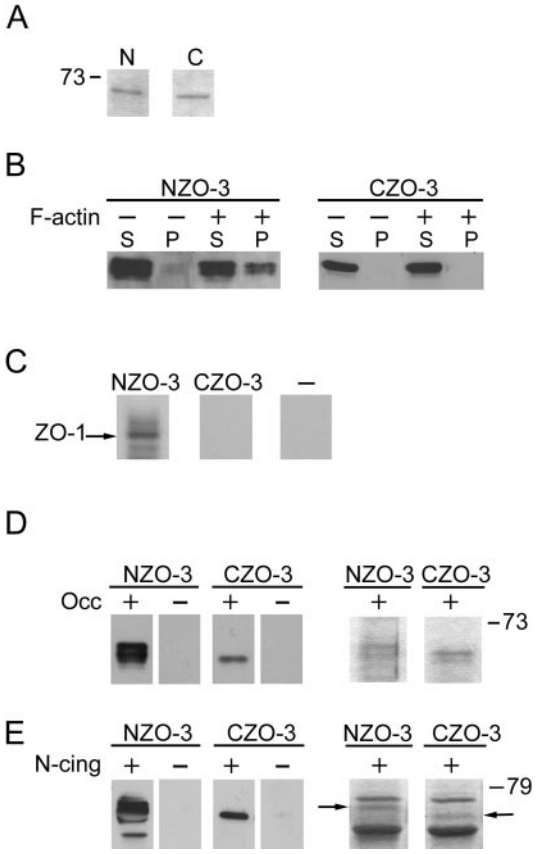

Figure 10. In vitro binding analyses show that NZO-3 binds F-actin and ZO-1 exclusively; both NZO-3 and CZO-3 bind occludin and cingulin. (A) Coomassie blue–stained gel showing the equivalent amounts of NZO-3 (N) and CZO-3 (C) fusion proteins used in all subsequent binding assays. (B) NZO-3 specifically cosediments with actin filaments; CZO-3 does not. Equivalent amounts of NZO-3 or CZO-3 were centrifuged in the presence (+) or absence (−) of F-actin. Stoichiometrically equivalent aliquots of supernatants (S) and pellets (P) were analyzed by immunoblot. NZO-3, but not CZO-3, is found in the F-actin pellet. (C) NZO-3 binds ZO-1; CZO-3 does not. ^{35}S-labeled in vitro–transcribed/translated ZO-1 was incubated with affinity resin containing equal amounts of NZO-3 or CZO-3. The 6-histidine tag plus 36 nonspecific amino acids served as negative control (−). As detected by autoradiogram, ZO-1 is retained by the NZO-3-containing resin and does not bind to CZO-3 or the negative control peptide. (D) Both halves of ZO-3 bind occludin with similar affinity. NZO-3 and CZO-3 were incubated with affinity resin containing immobilized GST-occludin (+), or GST alone (−). Bound protein was eluted with glutathione and analyzed by immunoblot with anti–ZO-3 antibodies (first four lanes) or Coomassie blue staining (last two lanes). Both NZO-3 and CZO-3 are retained by GST-occludin and not by GST alone. The Coomassie blue–stained lanes show that approximately equal amounts of NZO-3 and CZO-3 (arrows) are bound. (E) Both halves of ZO-3 bind to the amino-terminal head region of cingulin. NZO-3 or CZO-3 were added to an affinity column containing the amino-terminal head region of cingulin (N-cing) fused to GST (+) or GST alone (−). Bound fractions were immunoblotted with antibodies specifically recognizing NZO-3 or CZO-3 (first four lanes) or stained with Coomassie blue (last two lanes). Both NZO-3 and CZO-3 are retained on the GST–N-cingulin column but not on GST alone. Coomassie blue staining of the bound fractions shows approximately equal amounts of NZO-3 or CZO-3 (arrows) are bound. The other protein bands visible in the Coomassie blue–stained samples correspond to GST–N-cingulin.

experiments revealed that the PDZ domain-containing amino-terminal half of ZO-3 binds to ZO-1 and F-actin, whereas both halves of ZO-3 appear to bind occludin and cingulin. These results suggest that a mechanism involving assembly of the actin cytoskeleton at the junctional membrane mediated through ZO-3 and/or ZO-1 underlies the inhibition of junctional assembly by NZO-3.

The amino-terminal half of ZO-3 contains three PDZ domains, an arginine-rich domain and a proline-rich region. This portion of the molecule correctly localizes to the TJ, whereas the carboxy-terminal half, which contains the SH3 domain, GUK domain, and acidic region, remains diffusely distributed in the cytoplasm. This is in contrast to the findings for ZO-1, where it was shown that the region encompassing the GUK and acidic region is required for correct targeting (Fanning et al., 1998). Furthermore, when just the three PDZ domains of ZO-1 were expressed in MDCK cells, this construct failed to localize to the TJ (Reichert et al., 2000) and induced an epithelial to mesenchymal transition. Our results indicate that the PDZ domain-containing region of ZO-3 contains functional characteristics distinct from those of ZO-1.

Physiological data pertaining to the formation of the TJ barrier during junction assembly was obtained by using TER as an indicator of TJ integrity. Exogenous expression of NZO-3, CZO-3, or FLZO-3 did not alter steady-state TER levels (data not shown). However, when TER was measured during the time course of de novo TJ assembly in the calcium switch experimental system, it became apparent that expression of NZO-3 exerted a dominant-negative effect. Whereas CZO-3 or FLZO-3 expression did not affect TER recovery after calcium switch compared with untransfected parental MDCK cells, a calcium switch–induced increase in NZO-3 expression caused a significant lag in TER recovery after the re-addition of calcium (Fig. 3 A). It was not until 48 h that MDCK/NZO-3 cells approached the TER levels of the other cell lines, an effect that temporally correlated with the return of NZO-3 expression to steady-state levels. The fact that steady-state TER levels were not affected by steady-state NZO-3 expression indicates that this construct exerts its effect only at the higher expression levels induced by the calcium switch and/or specifically during the assembly process, although it can not be ruled out that other undetected phenotypic alterations may be occurring.

We used recovery from cD treatment as a second TJ assembly paradigm, and these experiments corroborated the calcium switch results. When parental cells or cell lines expressing FLZO-3, NZO-3, or CZO-3 were treated with the actin-disrupting drug, all showed the expected immediate drops in TER. However, when cD was washed out, the MDCK/NZO-3 cells displayed a lag in TER recovery (Fig. 3 B). These results are consistent with the hypothesis that the NZO-3 construct exerts its effects on junction assembly through interactions with the actin cytoskeleton.

An unexpected result of NZO-3 expression during the calcium switch experiment was that AJ formation, as assessed by localization of E-cadherin (Fig. 7) and β-catenin (Fig. 8) to cell borders, was also delayed. The current model of junctional complex assembly in polarized epithelial cells is based on the discovery that E-cadherin–mediated cell adhesion provides the initial step that must occur before TJs can form (Gumbiner et al., 1988). Our data support the novel concept that exogenous expression of a truncated TJ protein component can exert effects on the AJ-associated proteins E-cadherin and β-catenin. The fact that both TJ and AJ proteins are similarly delayed in their assembly at the membrane lends credence to the notion that the two types of junctions share a coordinated assembly process, and that NZO-3 affects one or more steps in this process.

Immunofluorescence localization experiments showed that the TJ proteins ZO-1, ZO-2, endogenous ZO-3, and occludin, and the AJ proteins E-cadherin and β-catenin were mislocalized during the early stages of junction assembly after calcium switch (Figs. 4, 7, 8, and data not shown). Moreover, the recovery of the typical localization of these proteins at cell borders temporally correlated with TER recovery after calcium switch. The fact that at later time points the cells were able to overcome the inhibitory effect exerted by NZO-3, as determined by the recovery of TER and correct targeting of ZO-1, ZO-2, ZO-3, occludin, E-cadherin and β-catenin to cell–cell contacts, is likely due to the observed return of NZO-3 protein expression to steady-state levels at later time points (Fig. 9 A). The mechanism(s) by which the calcium switch treatment causes NZO-3 expression to increase and then return to stable, steady-state levels is not known, although the effect was observed in repeated experiments with the same cell line (data not shown). Regardless, our results demonstrate that the NZO-3 construct has a dominant-negative effect on junctional complex assembly.

Immunofluorescence staining of the NZO-3 construct was faint at the later time points, likely due to the lower levels of NZO-3 expression. We did not try to boost expression levels with sodium butyrate because such treatment was toxic to the cells after periods longer than overnight, and overnight pulses of sodium butyrate treatment during calcium switch caused TER levels in parental cells to fluctuate significantly (data not shown). In addition, the anti-VSVG antibody only weakly reacted with our epitope-tagged construct in immunofluorescence and exhibited nonspecific nuclear staining, making it difficult to interpret the finer details of NZO-3 localization. However, we were able to determine that NZO-3 colocalizes with ZO-1 at cell borders at more mature TJs during calcium switch (Fig. 5). The NZO-3 construct did not colocalize with ZO-1 in the large intracellular aggregates that were observed in cells lacking cell border staining or with thick bars of ZO-1 at single cell–cell contacts that may represent two adjacent cells beginning TJ formation (Fig. 5). Because of the high nonspecific background staining, it is difficult to see whether another pool of NZO-3 exists in the cytoplasm. Based on the data presented here, and by confocal Z-section analysis which shows precise colocalization of NZO-3 and ZO-1 at the TJ and no overlap of NZO-3 with E-cadherin more basally situated along the lateral membrane (data not shown), we believe the NZO-3 construct is not found at the AJ in the calcium switch.

The involvement of the actin cytoskeleton in maintaining TJ integrity and regulating permeability has been well documented; this involvement is underscored by the fact that actin has multiple protein binding partners at the TJ (Itoh et al., 1997; Fanning et al., 1998; Wittchen et al., 1999), which themselves interact in various ways. It can be envisioned that this molecular architecture provides the

means by which an actin filament network can be recruited to and organized in a functionally relevant manner at the TJ. The actin cytoskeleton is also a major structural and functional element of the AJ (Farquhar and Palade, 1963; Rimm et al., 1995; Yonemura et al., 1995), and is present in a bundled actin belt around the apical periphery cell at the level of the AJ. Interestingly, in MDCK/NZO-3 cells, there is a delay in actin recruitment and formation of this perijunctional apical actin ring (Fig. 6). Because the amino-terminal half of ZO-3 is responsible for binding F-actin, this may represent one mechanism whereby expression of this construct affects TJ and AJ assembly.

Not only did expression of the amino terminus of ZO-3 alter the distribution of β-catenin, but there was also an increase in the TX-100–soluble pool of signaling-active β-catenin. Presumably the presence of an increased level of the NZO-3 construct at early time points after calcium switch results in a downstream alteration of the E-cadherin/catenins complex at the adherens junction, releasing β-catenin from a cytoskeletal linkage into the TX-100–soluble pool. A corresponding change in the levels of β-catenin in the insoluble pool is not observed, although any possible change may be masked by the overall high levels of β-catenin present in these samples. Normally cytoplasmic β-catenin levels are strictly regulated via a ubiquitin-mediated proteolysis pathway requiring β-catenin interaction with the cytoplasmic tumor suppressor APC (Aberle et al., 1997). Soluble β-catenin that escapes this targeted proteolysis is capable of translocating to the nucleus where it acts as a transcriptional transactivator in a complex with TCF/LEF family of transcription factors to direct transcription of a variety of genes that promote a proliferative phenotype (Behrens et al., 1996; Huber et al., 1996; Tetsu and McCormick, 1999). Recently, Stewart et al. (2000), showed that expression of a mutant signaling-active (soluble) form of β-catenin in MDCK cells caused a delay in the establishment of tight confluent cell monolayers compared with control cells, and the cells appeared more motile and formed less compact colonies when plated at a low density. These results, taken together with our data showing that NZO-3 expression delays TER formation after a calcium switch and results in an increased level of signaling-active, soluble β-catenin in these cells, suggests that NZO-3 might act through β-catenin to exert its effects on epithelial junctional complex formation. At present we do not know if this action is direct or indirect.

In summary, through these studies we attempted to further elucidate the role of ZO-3 in epithelial cell physiology, including the role it plays in junctional complex assembly and its protein binding interactions. Exogenous expression of partial constructs is the experimental method we chose to approach the dissection of ZO-3 protein function and TJ physiology. This study demonstrates that exogenous expression of the PDZ domain-containing amino-terminal half of ZO-3 perturbs both TJ and AJ assembly. Moreover, expression of NZO-3 alters actin dynamics and increases the amount of soluble signaling-active β-catenin. We are currently testing the hypothesis that NZO-3 exerts its effect on junctional assembly via a mechanism that involves its F-actin and ZO-1 binding ability and/or the increase in soluble β-catenin.

This paper is dedicated to the memory of Bernie Gilula. His contributions to both our understanding of the tight junction and the career of B.R. Stevenson were considerable. Cell biology has lost a friend.

We thank Alan Fanning, Warren Gallin, Barry Gumbiner, Lijie Gu, Tom Hobman, Brigitte Keon, Carolyn Machamer, Manijeh Pasdar, Sandra Citi, and Alpha Yap for providing reagents and/or advice. We also thank Naveen Basappa for his expert assistance in this project.

This work was supported by grants from the Medical Research Council of Canada, the Kidney Foundation of Canada, and the Canadian Association of Gastroenterology/Janssen-Ortho Inc. E.S. Wittchen holds a Medical Research Council studentship.

Submitted: 18 July 2000
Revised: 14 September 2000
Accepted: 4 October 2000

References

Aberle, H., A. Bauer, J. Stappert, A. Kispert, and R. Kemler. 1997. Beta-catenin is a target for the ubiquitin-proteasome pathway. *EMBO (Eur. Mol. Biol. Organ.) J.* 16:3797–3804.

Anderson, J.M., B.R. Stevenson, L.A. Jesaitis, D.A. Goodenough, and M.S. Mooseker. 1988. Characterization of ZO-1, a protein component of the tight junction from mouse liver and Madin-Darby canine kidney cells. *J. Cell Biol.* 106:1141–1149.

Ando-Akatsuka, Y., S. Yonemura, M. Itoh, M. Furuse, and S. Tsukita. 1999. Differential behavior of E-cadherin and occludin in their colocalization with ZO-1 during the establishment of epithelial cell polarity. *J. Cell Physiol.* 179:115–125.

Bazzoni, G., O.M. Martinez-Estrada, F. Orsenigo, M. Cordenonsi, S. Citi, and E. Dejana. 2000. Interaction of Junctional Adhesion Molecule with the tight junction components ZO-1, cingulin, and occludin. *J. Biol. Chem.* 275: 20520–20526.

Beatch, M., L.A. Jesaitis, W.J. Gallin, D.A. Goodenough, and B.R. Stevenson. 1996. The tight junction protein ZO-2 contains three PDZ (PSD-95/Discs-large/ZO-1) domains and an alternatively spliced region. *J. Biol. Chem.* 271: 25723–25726.

Behrens, J., J.P. von Kries, M. Kuhl, L. Bruhn, D. Wedlich, R. Grosschedl, and W. Birchmeier. 1996. Functional interaction of beta-catenin with the transcription factor LEF-1. *Nature.* 382:638–642.

Cereijido, M., E.S. Robbins, W.J. Dolan, C.A. Rotunno, and D.D. Sabatini. 1978. Polarized monolayers formed by epithelial cells on permeable and translucent support. *J. Cell Biol.* 77:853–880.

Cordenonsi, M., F. D'Atri, E. Hammar, D.A. Parry, J. Kendrick-Jones, D. Shore, and S. Citi. 1999. Cingulin contains globular and coiled-coil domains and interacts with ZO-1, ZO-2, ZO-3, and myosin. *J. Cell Biol.* 147:1569–1582.

Fagotto, F., N. Funayama, U. Gluck, and B.M. Gumbiner. 1996. Binding to cadherins antagonizes the signaling activity of beta-catenin during axis formation in Xenopus. *J. Cell Biol.* 132:1105–1114.

Fanning, A.S., B.J. Jameson, L.A. Jesaitis, and J.M. Anderson. 1998. The tight junction protein ZO-1 establishes a link between the transmembrane protein occludin and the actin cytoskeleton. *J. Biol. Chem.* 273:29745–29753.

Farquhar, M.G., and G.E. Palade. 1963. Junctional complexes in various epithelia. *J. Cell Biol.* 17:375–412.

Funayama, N., F. Fagotto, P. McCrea, and B.M. Gumbiner. 1995. Embryonic axis induction by the armadillo repeat domain of beta-catenin: evidence for intracellular signaling. *J. Cell Biol.* 128:959–968.

Furuse, M., T. Hirase, M. Itoh, A. Nagafuchi, S. Yonemura, Sa. Tsukita, and Sh. Tsukita. 1993. Occludin: a novel integral membrane protein localizing at tight junctions. *J. Cell Biol.* 123:1777–1788.

Furuse, M., M. Itoh, T. Hirase, A. Nagafuchi, S. Yonemura, Sa. Tsukita, and Sh. Tsukita. 1994. Direct association of occludin with ZO-1 and its possible involvement in the localization of occludin at tight junctions. *J. Cell Biol.* 127: 1617–1626.

Gumbiner, B., and K. Simons. 1986. A functional assay for proteins involved in establishing an epithelial occluding barrier: identification of an uvomorulin-like polypeptide. *J. Cell Biol.* 102:457–468.

Gumbiner, B., B.R. Stevenson, and A. Grimaldi. 1988. The role of the cell adhesion molecule uvomorulin in the formation and maintenance of the epithelial junctional complex. *J. Cell Biol.* 107:1575–1587.

Haskins, J., L. Gu, E.S. Wittchen, J. Hibbard, and B.R. Stevenson. 1998. ZO-3, a novel member of the MAGUK protein family found at the tight junction, interacts with ZO-1 and occludin. *J. Cell Biol.* 141:199–208.

Hirokawa, N., and L.G. Tilney. 1982. Interactions between actin filaments and membranes in quick-frozen and deeply etched hair cells of the chick ear. *J. Cell Biol.* 95:249–261.

Howarth, A.G., M.R. Hughes, and B.R. Stevenson. 1992. Detection of the tight junction-associated protein ZO-1 in astrocytes and other nonepithelial cell types. *Am. J. Physiol.* 262:C461–C469.

Huber, O., R. Korn, J. McLaughlin, M. Ohsugi, B.G. Herrmann, and R. Kemler. 1996. Nuclear localization of beta-catenin by interaction with transcription factor LEF-1. *Mech. Dev.* 59:3–10.

Itoh, M., A. Nagafuchi, S. Moroi, and S. Tsukita. 1997. Involvement of ZO-1 in cadherin-based cell adhesion through its direct binding to alpha catenin and actin filaments. *J. Cell Biol.* 138:181–192.

Itoh, M., M. Furuse, K. Morita, K. Kubota, M. Saitou, and S. Tsukita. 1999a. Direct binding of three tight junction-associated MAGUKs, ZO-1, ZO-2, and ZO-3, with the COOH termini of claudins. *J. Cell Biol.* 147:1351–1363.

Itoh, M., K. Morita, and S. Tsukita. 1999b. Characterization of ZO-2 as a MAGUK family member associated with tight as well as adherens junctions with a binding affinity to occludin and alpha catenin. *J. Biol. Chem.* 274: 5981–5986.

Jesaitis, L.A., and D.A. Goodenough. 1994. Molecular characterization and tissue distribution of ZO-2, a tight junction protein homologous to ZO-1 and the drosophila discs-large tumor suppressor protein. *J. Cell Biol.* 124:949–961.

Madara, J.L. 1987. Intestinal absorptive cell tight junctions are linked to cytoskeleton. *Am. J. Physiol.* 253:C171–C175.

Madara, J.L., D. Barenberg, and S. Carlson. 1986. Effects of cytochalasin D on occluding junctions of intestinal absorptive cells: further evidence that the cytoskeleton may influence paracellular permeability and junctional charge selectivity. *J. Cell Biol.* 102:2125–2136.

Madara, J.L., and J.R. Pappenheimer. 1987. Structural basis for physiological regulation of paracellular pathways in intestinal epithelia. *J. Membr. Biol.* 100:149–164.

Morita, K., M. Furuse, K. Fujimoto, and S. Tsukita. 1999. Claudin multigene family encoding four-transmembrane domain protein components of tight junction strands. *Proc. Natl. Acad. Sci. USA.* 96:511–516.

Rajasekaran, A.K., M. Hojo, T. Huima, and E. Rodriguez-Boulan. 1996. Catenins and zonula occludens-1 form a complex during early stages in the assembly of tight junctions. *J. Cell Biol.* 132:451–463.

Reichert, M., T. Muller, and W. Hunziker. 2000. The PDZ domains of zonula occludens-1 induce an epithelial to mesenchymal transition of Madin-Darby canine kidney I cells. Evidence for a role of beta-catenin/Tcf/Lef signaling. *J. Biol. Chem.* 275:9492–9500.

Rimm, D.L., E.R. Koslov, P. Kebriaei, C.D. Cianci, and J.S. Morrow. 1995. Alpha 1(E)-catenin is an actin-binding and -bundling protein mediating the attachment of F-actin to the membrane adhesion complex. *Proc. Natl. Acad. Sci. USA.* 92:8813–8817.

Sakakibara, A., M. Furuse, M. Saitou, Y. Ando-Akatsuka, and Sh. Tsukita. 1997. Possible involvement of phosphorylation of occludin in tight junction formation. *J. Cell Biol.* 137:1393–1401.

Stevenson, B.R., and D.A. Begg. 1994. Concentration-dependent effects of cytochalasin D on tight junctions and actin filaments in MDCK epithelial cells. *J. Cell Sci.* 107:367–375.

Stevenson, B.R., J.D. Siliciano, M.S. Mooseker, and D.A. Goodenough. 1986. Identification of ZO-1: a high molecular weight polypeptide associated with the tight junction (zonula occludens) in a variety of epithelia. *J. Cell Biol.* 103:755–766.

Stewart, D.B., A.I. Barth, and W.J. Nelson. 2000. Differential regulation of endogenous cadherin expression in Madin-Darby Canine Kidney cells by cell–cell adhesion and activation of beta-catenin signaling. *J. Biol. Chem.* 275: 20707–20716.

Takakuwa, R., Y. Kokai, T. Kojima, T. Akatsuka, H. Tobioka, N. Sawada, and M. Mori. 2000. Uncoupling of gate and fence functions of MDCK cells by the actin-depolymerizing reagent mycalolide B. *Exp. Cell Res.* 257:238–244.

Tetsu, O., and F. McCormick. 1999. Beta-catenin regulates expression of cyclin D1 in colon carcinoma cells. *Nature.* 398:422–426.

Troxell, M.L., S. Gopalakrishnan, J. McCormack, B.A. Poteat, J. Pennington, S.M. Garringer, E.E. Schneeberger, W.J. Nelson, and J.A. Marrs. 2000. Inhibiting cadherin function by dominant mutant E-cadherin expression increases the extent of tight junction assembly. *J. Cell Sci.* 113:985–996.

Wittchen, E.S., J. Haskins, and B.R. Stevenson. 1999. Protein interactions at the tight junction. Actin has multiple binding partners, and ZO-1 forms independent complexes with ZO-2 and ZO-3. *J. Biol. Chem.* 274:35179–35185.

Wong, V., and B.M. Gumbiner. 1997. A synthetic peptide corresponding to the extracellular domain of occludin perturbs the tight junction permeability barrier. *J. Cell Biol.* 136:399–409.

Yamamoto, T., N. Harada, K. Kano, S.-I. Taya, E. Canaani, Y. Matsuura, A. Mizoguchi, C. Ide, and K. Kaibuchi. 1997. The ras target AF-6 interacts with ZO-1 and serves as a peripheral component of tight junctions in epithelial cells. *J. Cell Biol.* 139:785–795.

Yonemura, S., M. Itoh, A. Nagafuchi, and Sh. Tsukita. 1995. Cell-to-cell adherens junction formation and actin filament organization: similarities and differences between non-polarized fibroblasts and polarized epithelial cells. *J. Cell Sci.* 108:127–142.